Mass transport behavior of polypyrrole and poly(*N*-methylpyrrole) films in acetonitrile solutions☆

Hochun Lee, Haesik Yang, Juhyoun Kwak *

Department of Chemistry, Korea Advanced Institute of Science and Technology, Taejon 305-701, South Korea

Abstract

The mass transport mechanism of polypyrrole (PPy) and poly(*N*-methylpyrrole) (PMPy) films in an acetonitrile (AN) solution has been investigated with the cyclic electrochemical quartz crystal microbalance (EQCM) technique. Cations as well as anions take part in ion transport during the redox reaction of PPy films, and the break-in process occurs in the first negative scan. On the other hand, anion transport is dominant during the redox reaction of PMPy films, and no break-in process is observed. Solvent transport takes place in the same direction as cation transport in the case of PPy films, whereas it occurs in the opposite direction to anion transport in the case of PMPy films. © 1999 Elsevier Science S.A. All rights reserved.

Keywords: EQCM; Polypyrrole; Poly(*N*-methylpyrrole); Ion transport; Solvent transport

1. Introduction

Mass transport of electrolyte species during the redox reaction of conducting polymers, plays an important role in determining their electrochemical characteristics, and has been extensively investigated by many groups [1,2]. In general, the mass transport mechanism is very complex, because dual ion transport, solvent transport, and neutral salt transport are present and they depend on the applied potential. In spite of these complexities, considerable progress has been made in the elucidation of the mass transport mechanism in an aqueous solution. Recently, we reported valuable information on water transport in polypyrrole (PPy) and poly(*N*-methylpyrrole) (PMPy) films [3,4]. We showed that water transport accompanying cation transport in a PPy film depends on the nature and concentration of the electrolyte solution as well as the applied potential. We also showed that water transport during anion transport in a PMPy film does not change extensively with the concentration of the electrolyte solution and the applied potential. Moreover, it was found that the amount of accompanying water per ion affects the ionic conductivity in the film and the morphology change of a film.

Although the mass transport study of conducting polymers in polar aprotic solvents has been an important topic because of Li battery application [5,6], the study in such solvents has not been performed as extensively as in aqueous solutions. Daifuku et al. [7,8] reported that only anion transport occurs during the redox reaction of polyaniline (PAn) films in acetonitrile (AN) containing $LiClO_4$. Desilvestro et al. [9] showed that some propylene carbonate (PC) molecules move in the same or in the opposite direction with respect to anion transport during the redox reaction of PAn films in a PC solution. Hillman et al. [10] insisted that a neutral salt as well as an anion and a solvent take part in mass transport of polybithiophene films in AN. Schiavon et al. [11] showed that ion transport is anion-specific in the case of poly(*N*-alkyl-substituted pyrrole)

---

* Corresponding author. Tel.: + 82-42-869-2833; fax: + 82-42-869-2810.
 E-mail address: jhkwak@cais.kaist.ac.kr (J. Kwak)

films in an AN solution and that some AN molecules move in the opposite direction to anion transport. Thus, mass transport in an aprotic solvent is very complex, and its mechanism is still far from being fully understood.

In this study, the ion and solvent transport behavior for PPy and PMPy films in AN are investigated by using the cyclic electrochemical quartz crystal microbalance (EQCM) technique [12,13]. First, cyclic voltammograms and mass change diagrams are obtained for PPy and PMPy films during the first negative scan as well as the steady-state scan. Second, the identity of charge compensating species in various electrolyte solutions is revealed by quantitative analysis. Finally, the differences in the mass transport behavior between a PPy film and a PMPy film are discussed focusing on solvent transport.

2. Experimental

2.1. Chemicals

Pyrrole, N-methylpyrrole, and AN (anhydrous, 99.8%) were purchased from Aldrich and used as received. All the electrolytes used in this study are of reagent grade and were dried at 80°C under vacuum before use.

2.2. Electrochemistry and film preparations

A standard three-electrode cell was used for all electrochemical measurement with an $Ag \mid Ag^+$ (0.01 M $AgNO_3$ in AN) reference electrode and a Pt wire counter electrode. All potentials are quoted against the saturated calomel electrode (SCE). A 6 MHz AT-cut quartz crystal (Inficon, NY) coated with Au, 0.32 cm² in area, served as the working electrode. The electromechanical impedance of the quartz crystal was measured using a Hewlett-Packard 4285A LCR meter. The experimental setup for the EQCM and the electromechanical impedance experiment was the same as that reported previously [3]. PPy films were prepared galvanostatically at 0.2 mA cm^{-2} in AN containing 0.1 M pyrrole and 0.1 M electrolyte, and PMPy was polymerized from an AN solution containing 0.1 M N-methylpyrrole and 0.1 M electrolyte. The electrolyte used in the polymerizations is a salt containing TEA$^+$ and the anion to be used in the cyclic EQCM experiment. The charge consumed during the polymerization was 300 mC cm^{-2} for all the films. After polymerization, the films were washed with pure AN and transferred into an Ar-filled glove box. All the cyclic EQCM experiments were performed in the glove box, and the electromechanical impedance experiments were performed in the atmosphere with a closed cell.
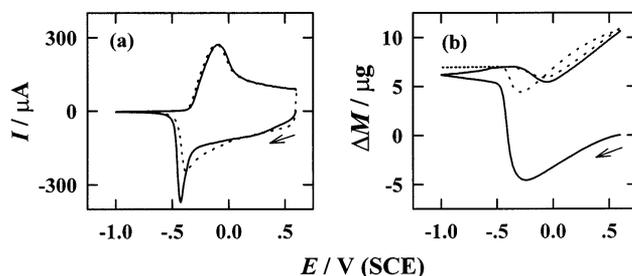

Fig. 1. (a) Cyclic voltammogram and (b) mass change diagram during the first (—) and second cycle (···) for a PPy film in 1 M LiClO$_4$ + AN, scan rate = 10 mV s^{-1}.

3. Results and discussion

3.1. Mass transport behavior in the first cathodic scan

Fig. 1 shows a cyclic voltammogram and a mass change diagram for a PPy film during the first two cycles in AN containing 1 M LiClO$_4$. The first negative scan exhibits a sharp and large peak at a more negative potential than that in the second scan. As shown in Fig. 1b, the mass of a film decreases at first and then increases sharply around the peak potential of the first negative scan. This means that anions initially move out of the film and that cations begin to move into the film around the peak potential. The charge change in the potential region where mass increases is 5.6 mC, which would correspond to 0.4 µg if only Li$^+$ insertion contributed to the mass increase. However, the actual mass change in this potential region is 10.7 µg. This large mass change indicates that there is considerable solvent transport in addition to Li$^+$ transport during the first negative scan.

On the contrary, in the case of a PMPy film, there is no significant difference between the first two cycles in both the cyclic voltammogram and the mass change diagram as shown in Fig. 2. Moreover, the mass of a film decreases monotonically in the negative scan and increases in the positive scan. It seems that anion transport is dominant over the whole scan range.
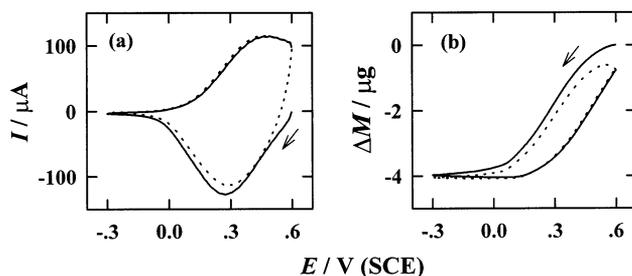

Fig. 2. (a) Cyclic voltammogram and (b) mass change diagram during the first (—) and second cycle (···) for a PMPy film in 1 M LiClO$_4$ + AN, scan rate = 10 mV s^{-1}.
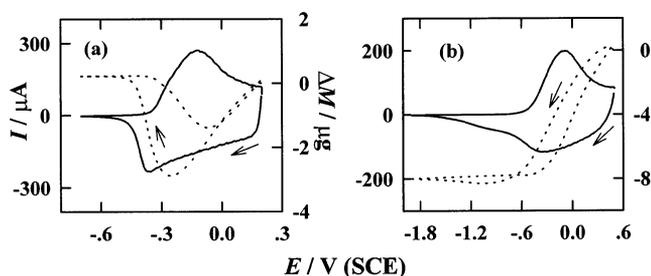
Fig. 3. Cyclic voltammogram (—) and mass change diagram (⋯) during the steady state for a PPy film in (a) 1 M LiClO$_4$ + AN and (b) 1 M TBAClO$_4$ + AN, scan rate = 10 mV s^{-1}.

The abnormal behavior in the first negative scan has been referred to as the 'break-in process.' It is known that the film after its deposition is compact [14]. When a cation with some solvent moves into the compact film in the first negative scan, the break-in process occurs [14,15]. However, when an anion moves out of the compact film, there is no break-in process. We reported previously that, in aqueous solutions, the break-in process is observed for a PPy/copper phthalocyaninetetrasulfonate film where cation transport is dominant [3], whereas it is not observed for a PMPy film where anion transport is dominant [4]. Thus, the break-in process in AN can be understood in the same way because the break-in process is observed for a PPy film where cation transport is considerable, whereas it is not observed for a PMPy film where only anion transport occurs.

3.2. Mass transport behavior in the steady state

Fig. 3a shows a cyclic voltammogram and a mass change diagram for a PPy film in LiClO$_4$ after the film has reached its steady state. Similar to the first negative scan (Fig. 1), the mass of a film decreases at first and then increases around the peak potential. This means that anion transport is dominant in the highly oxidized state of the film and that cation transport is dominant in its lightly oxidized state. Moreover, the extent of mass increase is significantly reduced when it is compared with that observed during the first scan. Fig. 3b shows the result obtained in TBAClO$_4$. When large TBA$^+$ is used as the electrolyte cation instead of small Li$^+$, the shape of the cyclic voltammogram is very different. The mass increase is very small in the lower potential region which means that cation transport is severely suppressed in the case of TBAClO$_4$. Consequently, it is evident that cation transport is considerable during the redox reaction of a PPy film.

Fig. 4a shows diagrams for a PMPy film in LiClO$_4$. The mass of a film decreases monotonically in the negative scan and increases in the positive scan, similarly to that of the first cycle (Fig. 2). Anion transport
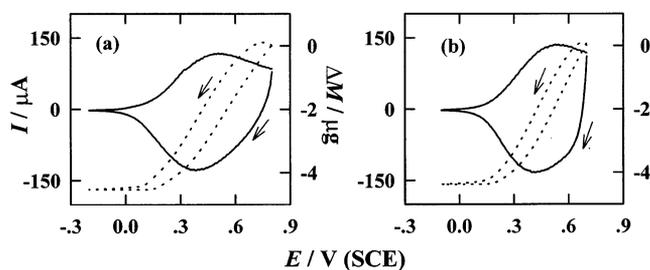
seems to be dominant over the whole range, too. Fig. 4b shows the result for a PMPy film in TBAClO$_4$. Contrary to PPy films, there is no significant change in the cyclic voltammogram or the mass change diagram when TBA$^+$ is used as the electrolyte cation instead of Li$^+$. Therefore, it is evident that cation transport is negligible during the redox reaction of a PMPy film.

3.3. Quantitative analysis

The plots of mass change (ΔM) vs. charge change (ΔQ) during the redox reaction of a PPy film (Fig. 3a) and a PMPy film (Fig. 4a) in 1 M LiClO$_4$ are shown in Figs. 5a,b, respectively. From the slope of the plot, the apparent molar mass (W') of charge compensating species can be calculated according to Eq. (1):

$$W' = -zF(\Delta M/\Delta Q) \tag{1}$$

where F is the Faraday constant and z is the electric charge of the charge compensating species.

3.3.1. PPy film

The ΔM vs. ΔQ plot for a PPy film (Fig. 5a) is V-shaped and exhibits 'hysteresis behavior'. Thus, we obtained two W' values for the oxidized and the reduced state. Because the value for the oxidized state is mainly related to anion transport, we represented it as W'_+. On the contrary, the value for the reduced state is represented as W'_- because it is mainly related to

Fig. 4. Cyclic voltammogram (—) and mass change diagram (⋯) during the steady state for a PMPy film in (a) 1 M LiClO$_4$ + AN and (b) 1 M TBAClO$_4$ + AN, scan rate = 10 mV s^{-1}.
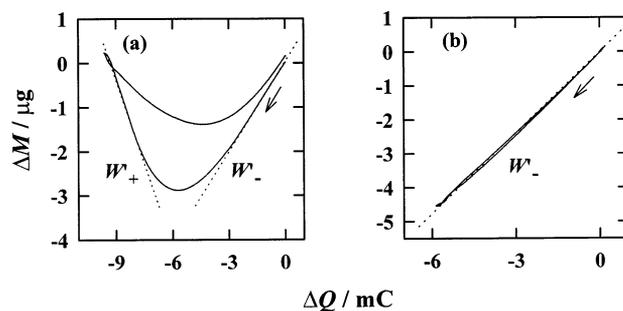

Fig. 5. Plots of mass change vs. charge change obtained from (a) Fig. 3a and (b) Fig. 4a.

Table 1
W' obtained from cyclic EQCM experiments for PPy films in AN

| Electrolyte | W_+^a | First scan | | | Steady-state | |
		W'_+^b (Y_+^c)	W'_-^b	W'_+ (Y_+)	W'_-
1.0 M LiClO$_4$	7	262 (6.2)	64	120 (2.7)	64
1.0 M TEAClO$_4$	130	177 (1.1)	68	136 (0.1)	58
0.1 M TEAClO$_4$	130	198 (1.7)	98	177 (1.1)	96
1.0 M TBAClO$_4$	243		59		86

[a] Molar mass of the cation (g mol^{-1}).
[b] $W' = -zF(\Delta M/\Delta Q)$ during the negative scan (g mol^{-1}).
[c] $Y_+ = (W'_+ - W_+)/W_{AN}$; $W_{AN} = 41.1$.

cation transport. W' values obtained in various systems are shown in Table 1. For a PPy film in 1 M LiClO$_4$, W'_+ values both in the first scan and in the steady-state scan are much larger than the molar mass of Li$^+$ ($W_{Li+} = 7$). A similar behavior is observed for PPy films in 1 and 0.1 M TEAClO$_4$. Two explanations are possible for the difference between the molar mass of the cation (W_+) and the apparent molar mass (W'_+). One is neutral salt transport, and the other is solvent transport. However, the difference for 1 M TEAClO$_4$ in the first scan ($177-130 = 47$) is much smaller than that for 1 M LiClO$_4$ ($262-7 = 255$). The same behavior is observed in the steady-state scan. If neutral salt transport occurred, the differences were larger for TEAClO$_4$ due to its large molar mass. Moreover, the differences in 0.1 M TEAClO$_4$ are larger than those in 1 M TEAClO$_4$. However, this would be reversed if neutral salt transport was present because neutral salt transport occurs more extensively in more concentrated electrolyte solutions. Therefore, the difference between W_+ and W'_+ is likely to be due to solvent transport. If only cation transport and solvent transport occur, W'_+ can be expressed as follows:

$$W'_+ = W_+ + Y_+ W_s \qquad (2)$$

where W_+ and W_s are the molar masses of a cation and a solvent, respectively, and Y_+ is the number of accompanying solvent molecules per cation. As shown in Table 1, Y_+ values for 1 M LiClO$_4$ are 6.2 and 2.7 in the first and in the steady-state scan, respectively. This means the amount of accompanying solvent is larger in the first scan than in the steady-state scan. For 1 M TEAClO$_4$, Y_+ values are 1.1 and 0.1, which are much smaller than those for LiClO$_4$ This indicates that the amount of accompanying solvent depends on the kind of cation. In addition, the fact that Y_+ values for 0.1 M TEAClO$_4$ are larger than those for 1 M TEAClO$_4$ means that the amount of accompanying solvent depends on the concentration of the electrolyte solution. The increased Y_+ in a dilute solution can be explained by the fact that the solvation number of the

ion increases due to the increased dielectric constant in a dilute solution [3].

In every PPy film, W'_- is smaller than $W_{ClO_4^-}$ ($= 99.5$) and varies little in comparison with the variation of W'_+. It is difficult to give a clear explanation for the smaller value of W'_- compared to $W_{ClO_4^-}$. In addition to anion transport, cation and solvent transport might occur even in the region where anion transport is dominant.

3.3.2. PMPy film

The ΔM vs. ΔQ plot for a PMPy film (Fig. 5b) is linear over the whole charge range, and it shows no hysteresis behavior. Since W'_- in the first scan is similar to that in the steady-state scan within the experimental error, only W'_- in the steady-state scan is obtained (Table 2). In LiClO$_4$, W'_- is 76, which is smaller than $W_{ClO_4^-}$. All W'_- values in other solutions containing ClO$_4^-$ are smaller than $W_{ClO_4^-}$, too. Moreover, W'_- values are not significantly affected by the kind of cation nor by the concentration of the electrolyte. It shows that cation or neutral salt transport is negligible in ClO$_4^-$-containing solutions. Therefore, the possibility that the smaller W'_- is due to cation or neutral salt transport in the opposite direction to anion transport can be excluded. In that case, two possibilities remain. One is that solvent transport occurs in the opposite direction to anion (ClO$_4^-$) transport, and the other is that the morphology change of a film results in a miscalculation of ΔM. In order to examine the latter possibility, the electromechanical impedance [16–18] is measured for a PMPy film in 1 M TEAClO$_4$ (Fig. 6). In the electromechanical impedance experiment, the excitation signal (Fig. 6a) consists of successive potential steps. The resonance frequency of a quartz crystal (Δf_o), the maximum-conductance fre-

Table 2
W'_- obtained from cyclic EQCM experiments for PMPy films in AN

Electrolyte	W_+^a	W_-^b	W'_-^c	Y_-^d
1.0 M LiClO$_4$	7	99.5	76	−0.6
1.0 M NaClO$_4$	23		77	−0.6
0.5 M Ba(ClO$_4$)$_2$	137		78	−0.5
1.0 M TEAClO$_4$	133		76	−0.6
0.1 M TEAClO$_4$	133		78	−0.5
1.0 M TBAClO$_4$	243		81	−0.5
0.1 M TBAClO$_4$	243		81	−0.5
1.0 M THAClO$_4$	355		77	−0.6
0.5 M LiBF$_4$	7	86.8	67	−0.5
0.5 M TBABF$_4$	243		67	−0.5
0.5 M LiCF$_3$SO$_3$	7	149.1	110	−1.0
0.5 M TBACF$_3$SO$_3$	243		112	−0.9

[a] Molar mass of the cation (g mol^{-1}).
[b] Molar mass of the anion (g mol^{-1}).
[c] $W'_- = F(\Delta M/\Delta Q)$ during the negative scan (g mol^{-1}).
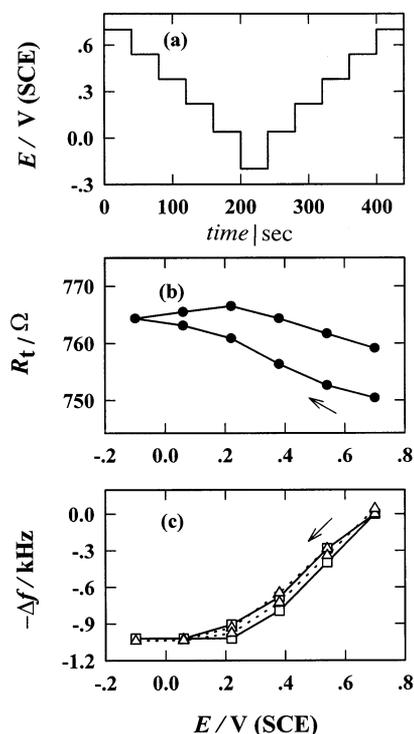[d] $Y_- = (W'_- - W_-)/W_{AN}$; $W_{AN} = 41.1$.

Fig. 6. (a) Applied potential vs. time, (b) R_t change, and (c) f_r (—□—), f_o (···△···) changes for a PMPy film in 1 M TEAClO$_4$ + AN during the electromechanical impedance experiment.

frequency (Δf_r), and the total resistance of a quartz crystal (R_t) are measured at every step after steady state is established. It has been known that Δf_r depends only on ΔM, and R_t depends on the morphology change of a film. We previously reported that the comparison between f_o and f_r enables one to verify the linear relation between ΔM and Δf_o [3]. As shown in Fig. 6b, R_t varies within about 20 Ω, which is very small compared with that for other systems reported previously [3]. It indicates that the morphology change is not significant during the redox reaction of a PMPy film in an AN solution. Moreover, the Δf_o behavior is very similar to the Δf_r behavior as shown in Fig. 6c. Therefore, ΔM can be obtained from Δf_o without considering a change in the morphology of the film in this system. Consequently, the smaller value of W'_- is related to solvent transport occurring in the opposite direction to anion transport. Assuming that only anion transport and solvent transport take place, W'_- can be expressed as below:

$$W'_- = W_- + Y_- W_s \qquad (3)$$

where W_- and W_s are the molar masses of an anion and a solvent, respectively, and Y_- is the number of accompanying solvent molecules per anion. As shown in Table 2, Y_- for PMPy films in ClO$_4^-$-containing AN is between -0.5 and -0.6. This means that some AN molecules (about 0.5 per ClO$_4^-$) move in the opposite direction to ClO$_4^-$ transport.

In order to examine the effect of the anion on the mass transport of a PMPy film, cyclic EQCM experiments were performed in solutions containing BF$_4^-$ and CF$_3$SO$_3^-$. The cyclic voltammograms and mass change diagrams are very similar to those of ClO$_4^-$-containing solutions. Table 2 shows that the W'_- value is 67 in both LiBF$_4$ and TBABF$_4$, and that the value is about 110 in both LiCF$_3$SO$_3$ and TBACF$_3$SO$_3$. It shows that W'_- values are smaller than W_- ($W_{BF_4^-} = 86.8$ and $W_{CF_3SO_3^-} = 149$) and independent of the kind of cation in both solutions containing BF$_4^-$ and CF$_3$SO$_3^-$. Thus, it is evident that cation or neutral salt transport is negligible and that counter flux of the solvent occurs in these solutions.

4. Conclusions

Ion and solvent transport behavior for PPy and PMPy films in AN was investigated with the cyclic EQCM technique. Cations as well as anions take part in ion transport during the redox reaction of PPy films, and AN transport also occurs in the same direction as cation transport. In the first negative scan, the break-in process takes place and AN molecules are inserted into the film. In a TBA$^+$-containing solution, cation transport is suppressed because of the large cation. On the other hand, anion transport is dominant during the redox reaction of PMPy films. AN transport takes place in the opposite direction to anion transport.

References

[1] G. Inzelt, in: A.J. Bard (Ed.), Electroanalytical Chemistry, vol. 18, Marcel Dekker, New York, 1994, p. 89.
[2] M.E.G. Lyons, in: M.E.G. Lyons (Ed.), Electroactive Polymer Electrochemistry, Part 1, Plenum, New York, 1994, p. 1.
[3] H. Yang, J. Kwak, J. Phys. Chem. B 101 (1997) 774.
[4] H. Yang, J. Kwak, J. Phys. Chem. B 101 (1997) 4656.
[5] T. Momma, K. Nishimura, T. Osaka, N. Kondo, S. Nakamura, J. Electrochem. Soc. 141 (1994) 2326.
[6] P. Novák, K. Müler, K.S.V. Santhanam, O. Haas, Chem. Rev. 97 (1997) 207.
[7] H. Daifuku, T. Kawagoe, N. Yamamoto, T. Ohsaka, N. Oyama, J. Electroanal. Chem. 274 (1989) 313.
[8] H. Daifuku, T. Kawagoe, T. Matsunaga, N. Yamamoto, T. Ohsaka, N. Oyama, Synth. Met. 41–43 (1991) 2897.
[9] J. Desilvestro, W. Scheifele, O. Hass, J. Electrochem. Soc. 139 (1992) 2727.
[10] A.R. Hillman, M.J. Swann, S. Bruckenstein, J. Electroanal. Chem. 291 (1990) 147.

[11] G. Schiavon, G. Zotti, N. Comisso, A. Berlin, G. Pagani, J. Phys. Chem. 102 (1992) 1982.

[12] D.A. Buttry, M.D. Ward, Chem. Rev. 92 (1992) 1355.

[13] D.A. Buttry, in: A.J. Bard (Ed.), Electroanalytical Chemistry, vol. 17, Marcel Dekker, New York, 1991, p. 1.

[14] Q. Pei, O. Inganäs, J. Phys. Chem. 97 (1993) 6034.

[15] P.T Varineau, D.A. Buttry, J. Phys. Chem. 91 (1987) 1292.

[16] S.J. Martin, V.E. Granstaff, G.C. Frye, Anal. Chem. 63 (1991) 2272.

[17] M. Yang, M. Thompson, Anal. Chem. 65 (1993) 1158.

[18] M.A.M. Noël, P.A. Topart, Anal. Chem. 66 (1994) 484.